Physica A 462 (2016) 492–507

Contents lists available at ScienceDirect

Physica A

journal homepage: www.elsevier.com/locate/physa

Multiscale multifractal time irreversibility analysis of stock markets

Chenguang Jiang, Pengjian Shang *, Wenbin Shi

Department of Mathematics, School of Science, Beijing Jiaotong University, Beijing 100044, PR China

HIGHLIGHTS

- The MMRA method which is based on statistical moments reflects the multifractal characteristics of stock indices.
- The MMRA method makes the time irreversibility analysis of the series precisely through the segmentation algorithm.
- The generalized Hurst exponents of stock indices obtained by our method provide new prospective of assessing the evolution stage of stock markets.

ARTICLE INFO

Article history:
Received 27 September 2015
Received in revised form 18 May 2016
Available online 22 June 2016

Keywords:
Multiscale multifractal time irreversibility analysis(MMRA)
Segment size
Statistical moments
Delayed Henon map
Binomial multifractal model
Stock markets

ABSTRACT

Time irreversibility is one of the most important properties of nonstationary time series. Complex time series often demonstrate even multiscale time irreversibility, such that not only the original but also coarse-grained time series are asymmetric over a wide range of scales. We study the multiscale time irreversibility of time series. In this paper, we develop a method called multiscale multifractal time irreversibility analysis (MMRA), which allows us to extend the description of time irreversibility to include the dependence on the segment size and statistical moments. We test the effectiveness of MMRA in detecting multifractality and time irreversibility of time series generated from delayed Henon map and binomial multifractal model. Then we employ our method to the time irreversibility analysis of stock markets in different regions. We find that the emerging market has higher multifractality degree and time irreversibility compared with developed markets. In this sense, the MMRA method may provide new angles in assessing the evolution stage of stock markets.

1. Introduction

Complexity, time irreversibility and fractal scaling characteristics reflect different aspects of nonlinear properties of living dynamical systems such as stock market fluctuations [1–4]. However, their joint analysis over the course of stock market is pending.

It is important to detect time asymmetry or irreversibility in nonstationary time series not only because time series may be easier to predict and model in one direction, but particularly because irreversibility is a symptom of non-Gaussian forcing and dynamic nonlinearities [5,6]. In addition, when time series represent the evolution of either stochastic or deterministic dynamical systems, irreversibility has a special meaning linked with the lack of equilibrium and detailed balance of the probability fluxes among the system states. Some notable work has been done in the analysis of time irreversibility [7–9].

* Corresponding author.
E-mail address: pjshang@bjtu.edu.cn (P.J. Shang).

http://dx.doi.org/10.1016/j.physa.2016.06.092
0378-4371/

In recent years, the Detrended Fluctuation Analysis (DFA) invented by Peng et al. [10] has been established as an effective tool for the detection of long-range (auto-) correlations in time series with non-stationarities. Then, in order to quantify long-range cross-correlations between two non-stationary time series, a new method named Detrended Cross-Correlation Analysis (DCCA), has been proposed recently. Many researchers have used DFA and DCCA in the time series analysis of various areas and have made great progress [11–16]. Its core algorithm of dividing the whole series into different segments, detrending fluctuation in every segment, and then utilizing the overall fluctuation function to study the long-range(auto-) correlations has inspired us a lot.

Detecting fractal properties of nonstationary time series is also of great significance [17–19]. In the case of monofractal time series, a single exponent H (the Hurst exponent) may be used to represent the fluctuation scaling [9]. However, there is a class of signals whose fractal properties vary from point to point along the time series [20]. Signals which require not only one but also a whole spectrum of local Hurst exponents h are so-called multifractal. More multifractal study details can be found in Refs. [21–26].

Stock markets delegate extremely complex systems with a large number of interacting units. The nature of these interactions and specially the mechanisms of influence of external factors vary from market to market. Nowadays, developed and emerging markets are in different evolution stage, but the variables generated by the underlying stochastic process, for example, the values of market indices may exhibit a universal behavior [27–29]. Studying the similarities and differences between these markets may provide constructive suggestion for the steady development of the global financial market.

Inspired by the segmentation algorithm of DFA, we develop a method called multiscale multifractal time irreversibility analysis (MMRA), which employs the segmentation algorithm into the analysis of time irreversibility to increase the accuracy and study the fractal properties of the time series. We test the effectiveness of MMRA in detecting multifractality and time irreversibility of time series generated from delayed Henon map and binomial multifractal model. Then we apply this method to stock markets in three different continents, Europe, Asia and US markets. Through the analysis of the composite index of these markets, we make a comparison to assess the evolution stage of market and put forward some suggestions that may be useful for the investment funds industry and portfolio and risk management purposes.

This paper is structured as follows: in Section 2 we put forward the multiscale multifractal time irreversibility analysis. In Section 3, we discuss the input parameters setting and present numerical results for artificial time series. In Section 4, we employ MMRA into stock markets and analyze the result. Finally, in Section 5, we make the conclusions.

2. Methodology

Time irreversibility or asymmetry, a fundamental property of disequilibrium systems, is related to the unidirectionality of the energy flow across the boundaries of the system [30]. In time series analysis, time irreversibility refers to the lack of invariance of the statistical properties of a signal under the operation of time reversal [31].

Costa et al. [8] quantify the degree of time irreversibility in three steps: a coarse-graining procedure, the computation of time irreversibility for each coarse-grained series, and the integration of the results obtained for a pre-defined range of scales. They analyze the time irreversibility of series as a whole. However, this kind of time irreversibility analysis maybe somewhat rough because that the time irreversibility of series may vary from point to point, which seems to be more complex. With reference to segmentation algorithm of DFA and the multifractal study in Refs. [10,21], we apply the segmentation algorithm into the analysis of the time irreversibility of series to increase the accuracy and study the fractal properties of series, which is called multiscale multifractal time irreversibility analysis (MMRA).

MMRA can be introduced as follows:

Step 1: Starting with a correlated time series $\{x(i)\}$, $i = 1, 2, \ldots, N$, where N is the length of series. Transform the series into a new time series of coarse-grained differences defined as:

$$y(k) = x(k + l) - x(k). \tag{1}$$

Here, we adopt $l = 1$ in the ordinary multiscale time irreversibility analysis.

Step 2: The coarse-grained time series $\{y(k)\}$, $k = 1, 2, \ldots, N - 1$ is divided into $N_s = \mathrm{int}(N - 1 \setminus s)$ non-overlapping windows of equal length s. Since the record length $N-1$ does not need to be a multiple of the considered time scale s, a short part at the end of $\{y(k)\}$ will remain in most cases. In order to have into account this part of the record, the same procedure is repeated, starting from the other end of the record. Thus, $2N_s$ windows are obtained.

Step 3: Calculate the local increase and decrease for every segment as follows:

$$P^{+}(v, s) = \frac{1}{s}\sum_{j=0}^{s} H[-y_{(v-1)s+j}]. \tag{2}$$

$$P^{-}(v, s) = \frac{1}{s}\sum_{j=0}^{s} H[y_{(v-1)s+j}] \tag{3}$$

for $v = 1, \ldots, N_s$ and

$$P^{+}(v, s) = \frac{1}{s}\sum_{j=0}^{s} H\{-y_{[N-1-(v-N_s)s+j]}\}. \tag{4}$$

$$P^{-}(v,s)=\frac{1}{s}\sum_{j=0}^{s}H\{y_{[N-1-(v-N_s)s+j]}\} \tag{5}$$

for $v=N_s+1,\ldots,2N_s$. Here, H is the Heaviside function ($H(a)=0$, if $a<0$ and $H(a)=1$, if $a\geq 0$). Consequently, $P^{+}(v,s)$ ranges from 0 to 1 and time irreversibility is characterized by values of $P^{+}(v,s)$ significantly larger or smaller than 0.5. $P^{+}(v,s)>0.5$ implies that the number of increments is larger than that of decrements.

For a perfectly symmetric time series, the number of increments is equal to the number of decrements. Thus, the time asymmetry can be defined at every scale as a difference between the percentages of increments and decrements [32]. For every segment v, the time irreversibility can be described as follows:

$$Ai(v,s)=P^{+}(v,s)-P^{-}(v,s). \tag{6}$$

Step 4: For time irreversibility of the coarse-grained time series $\{y(k)\}$ is evaluated by averaging over all local absolute time irreversibility in the vth window:

$$MsAi(s)=\frac{1}{2N_s}\sum_{v=0}^{2N_s}\left|Ai(v,s)\right|. \tag{7}$$

Step 5: The qth order time irreversibility is obtained by averaging over all segments:

$$MsAi_q(s)=\left\{\frac{1}{2N_s}\sum_{v=0}^{2N_s}\left|Ai(v,s)\right|^{q}\right\}^{\frac{1}{q}} \tag{8}$$

where, the index variable q can take any real value (for $q=0$, see Step 6). For $q=1$, we get the standard multiscale time irreversibility. We are interested in how the time irreversibility fluctuation function $MsAi_q(s)$ depend on the segment scale s for different values of q. Hence, we repeat Steps 2–5 for different segment scales s.

Step 6: Finally, the scaling behavior of time irreversibility is determined by analyzing log–log plots of $MsAi_q(s)$ vs. s for different values of q:

$$MsAi_q(s)\sim s^{h(q)}. \tag{9}$$

The value of $h(0)$, which corresponds to the limit $h(q)$ for $q\to 0$, cannot be determined directly using the averaging procedure in Eq. (8) because of the diverging exponent. Instead, a logarithmic averaging procedure has to be employed.

$$MsAi_0(s)=\exp\left\{\frac{1}{4N_s}\sum_{v=0}^{2N_s}\ln\left(\left|Ai(v,s)\right|\right)\right\}^{\frac{1}{q}}\sim s^{h(0)}. \tag{10}$$

For monofractal time series with compact support, $h(q)$ is independent of q, since the scaling behavior of $Ai(v,s)$ is identical for all segments, and the averaging procedure in Eq. (8) will give us this identical scaling behavior for all values of q. Only if small or large time irreversibility scales are different, there will be a significant dependence of $h(q)$ on q: if we consider positive values of q, the segment v with large time irreversibility $Ai(v,s)$ will dominate the average $MsAi_q(s)$. Thus, for positive values of q, $h(q)$ describes the scaling behavior of segments with large time irreversibility. On the contrary, for negative values of q, the segments v with small time irreversibility will dominate the average $MsAi_q(s)$. Hence, for negative values of q, $h(q)$ describes the scaling behavior of the segments with small time irreversibility.

3. Numerical results for artificial time series

3.1. How to set the input parameters scale and q in MMRA

The estimation of multiscale multifractal time irreversibility is dependent on these parameter settings. The input parameter scale is the multiple segment size for the computation of local time irreversibility. A minimum and maximum sample size of the segments has to be chosen to construct the set of scales used in MMRA. Both statistical and phenomenological arguments exist on how to choose the minimum and maximum segment size. The statistical argument is to choose minimum and maximum segment sizes that provide a numerical stable estimation of $MsAi_q$. The minimum segment sample size should be large enough to prevent error in the computation of local time irreversibility $Ai(v,s)$. For the computation of $Ai(v,s)$, a rule of thumb can be applied if the minimum segment size is larger than 10 samples. A maximum segment size below 1/10 of the sample size of the time series will provide at least 10 segments in the computation of $MsAi_q$. We have on average 3730 observations of every stock index. Furthermore, it is favorable to have a equal spacing between scales when they are represented in plot ($\log 2(scale)$, $\log 2(MsAi_q)$) to obtain a optimal performance of the linear regression that estimates q-order Hurst exponent $H(q)$. According to the above statements, we choose the minimum scale 2^4, the maximum scale 2^9, and the amount of scales is 40.

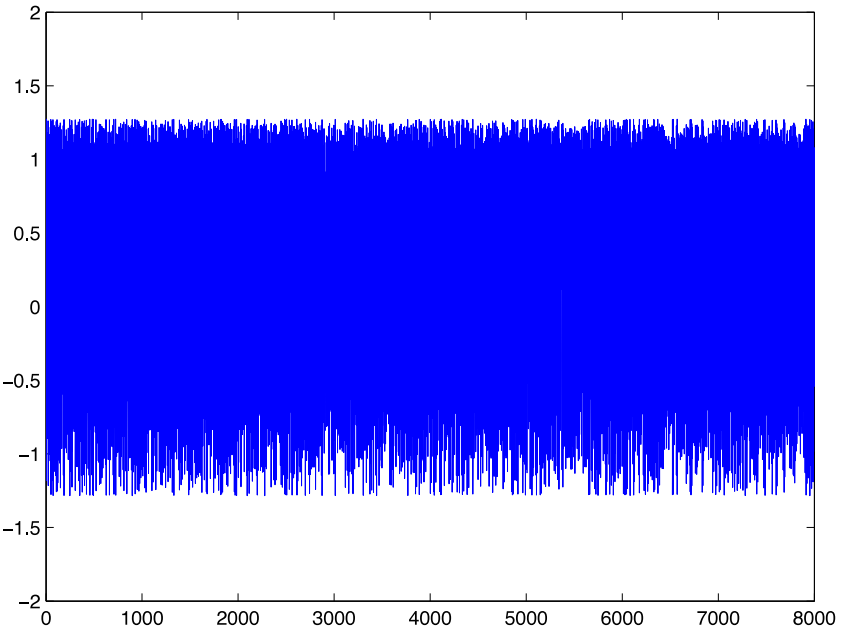

Fig. 1. Time series generated from zeroth-order *DHM*.

The input parameter q decides the q-order weighting of the local time irreversibility *MsAi* in MMRA. The q-order should consist of both positive and negative q in order to weight the periods with large and small time irreversibility in the time series. The precision of the computation of the q-order Hurst exponent $H(q)$ decreases with increasing negative and positive q-orders. The single segment with the smallest and largest time irreversibility *Ai* will tower up as a single skyscraper by increasing negative and positive q-orders, respectively, and completely dominate the scaling function $MsAi_q$. The choice of q-orders should therefore avoid large negative and positive values because they inflict larger numerical errors in the tails of the multifractal spectrum. A sufficient choice of q-orders will be between -5 and 5 for most nonstationary time series. Here, we consider 7 different q values, vary from -5 to 5 to include large and small time irreversibility in a time series.

3.2. Artificial time series based on the delayed Henon map

As a two dimensional mapping, Henon map is the simplest non-linearity mapping of high dimensional mappings. It can be denoted by the following formula:

$$\begin{cases} x(i+1) = 1 - ax^2(i) + y(i) \\ \qquad y(i+1) = bx(i). \end{cases} \tag{11}$$

When the parameter a takes 1.4 and the parameter b takes 0.3, the system turns into chaos. We use the delayed Henon map (DHM) to generate a set of time series to test the effectiveness of MMRA. The dynamics will be governed by a single parameter whose value determines the dimension of the system and hence its complexity. The system is algebraically minimal in that it has a single (quadratic) nonlinearity and a single linearity. The length of time series is 8000. The σ-order DHM can be written as:

$$\begin{cases} x(i+1) = 1 - ax^2(i-\sigma) + y(i-\sigma) \\ \qquad y(i+1) = bx(i-\sigma) \end{cases} \tag{12}$$

with $a = 1.4$, $b = 0.3$, and $i = \sigma + 1, \ldots, N - 1$. A non-delayed Henon map has $\sigma = 0$ and produces x that is found to be two irreversible. We set the initial values of the time series generated from zeroth-order *DHM* with $x(1) = 0.3$, $y(1) = 0.4$ and first-order *DHM* with $x(1) = 0.7$, $x(2) = 0.6$, $y(1) = 0.3$, $y(2) = 0.4$. Figs. 1 and 2 present time series generated from zeroth-order DHM and first-order DHM respectively.

Here, we give some basic statistical magnitudes of time series generated from zeroth-order DHM. The mean of the series is 0.2583, the standard deviation of the series is 0.72 and the skewness is -0.4986.

Similarly, we provide some basic statistical magnitudes of time series generated from first-order DHM. The mean of the series is 0.2609, the standard deviation of the series is 0.7183 and the skewness is -0.507.

We can see from Figs. 1 and 2, the basic statistical magnitudes of two series are similar, but we will dig more information from the time irreversibility analysis of the two series. In Figs. 3 and 4, we give the log–log plots of $MsAi_q$ vs. s for the data generated from zeroth-order *DHM* and first-order *DHM*.

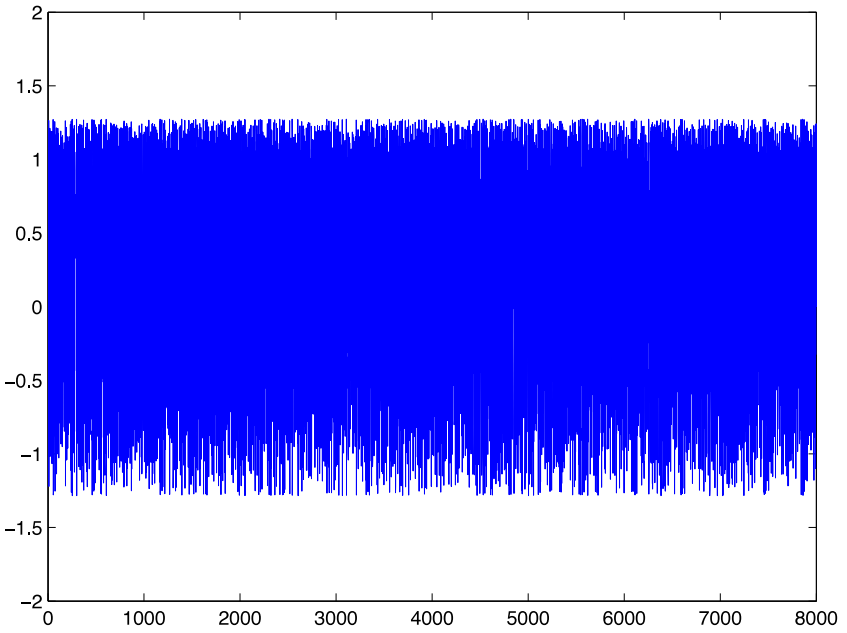

Fig. 2. Time series generated from first-order *DHM*.

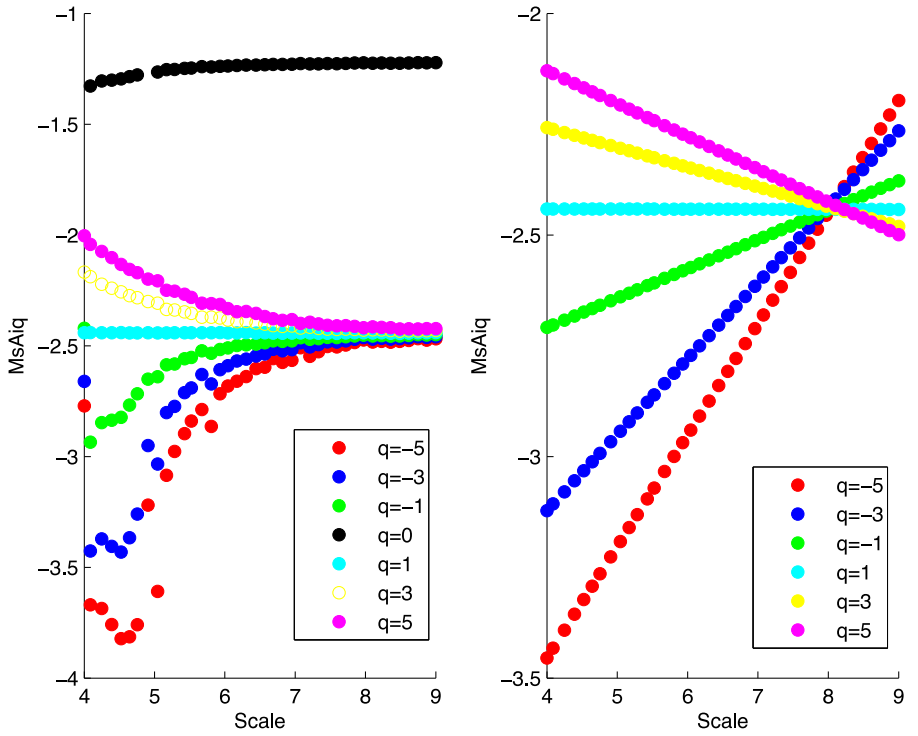

Fig. 3. The log–log plot of $MsAi_q$ vs. s of time series generated from zeroth-order *DHM*.

From Fig. 3, we can see that $MsAi_q$ generally fluctuates between 0.0707 and 0.2494 and converges to 0.1893 except for the case $q = 0$. When the parameter q takes zero, the fluctuation amplitude of $MsAi_q$ is small. Generally speaking, if $q < 0$, the fluctuation function $MsAi_q$ increases with the growth of the segment scale s; if $q > 0$, the fluctuation function $MsAi_q$ decreases as the scale s increases; if $q = 0$, the amplitude of fluctuation function $MsAiq$ is small. For the same segment scale, the larger the value of q (except $q = 0$), the larger value of fluctuation function $MsAi_q$. If the value of segment scale is large enough, the values of $MsAi_q$ tend to be same 0.1893. For different q and s, we have $MsAi_q \neq 0$, thus indicating that time series

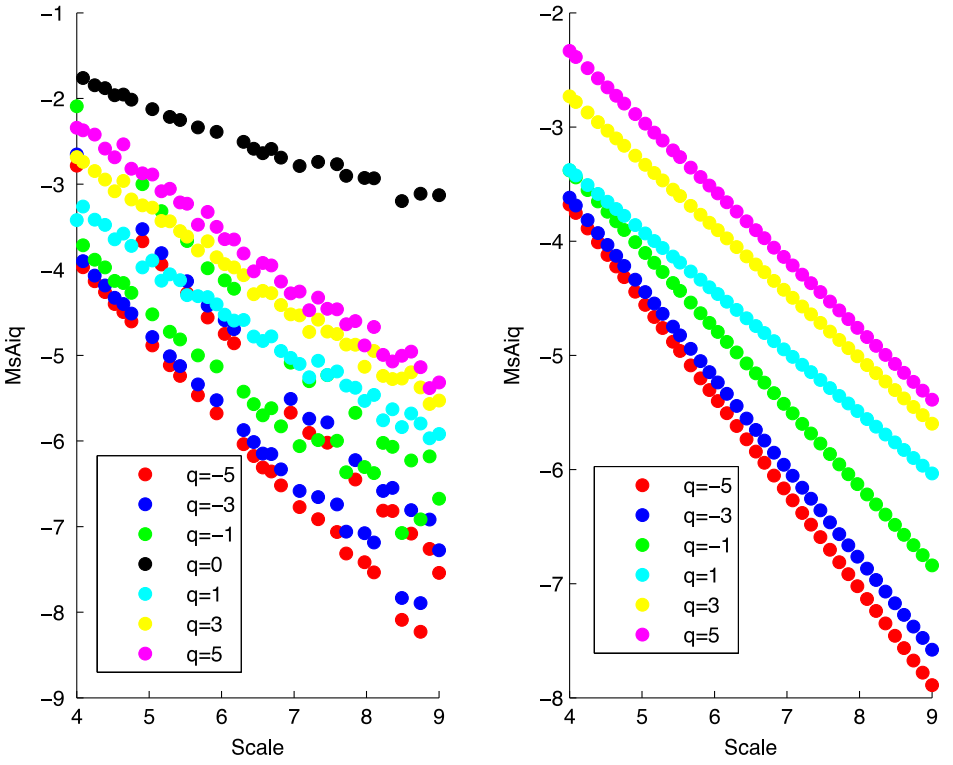

Fig. 4. The log–log plot of $MsAi_q$ vs. s of time series generated from first-order *DHM*.

is irreversible. The scaling behavior of $MsAi_q$ is apparent and there is a significant dependence of $h(q)$ on q, which reveals the multifractality of time irreversibility of the data generated from zeroth-order DHM.

As we can see from Fig. 4, if $q \neq 0$, the value of $MsAi_q$ generally fluctuates between 0.0035 and 0.2548. If $q = 0$, $MsAi_q$ undulates between 0 and 0.2548, whose fluctuate amplitude is relatively smaller than the case $q \neq 0$. Similarly, for different q and s, we have $MsAi_q \neq 0$, which indicating that time series is irreversible. No matter what the value of q is, $MsAi_q$ decreases with the growth of segment scale. When the segment size is fixed, $MsAi_q$ increases with the growth of statistical moments except $q = 0$. What is more, the trend of the fluctuation function $MsAi_q$ is more obvious comparing with the series generated from zeroth-order *DHM*. The different Hurst Exponent $H(q)$ for different q has certified the existence of multifractality.

As we can see from time irreversibility analysis of two series, the larger of the absolute of generalized Hurst exponent, the larger of the multifractality degree of the time series . Thus, time series generated from zeroth-order DHM has greater multifractality degree compared with time series generated from first-order DHM. Zeroth-order DHM time series have both positive and negative generalized Hurst exponents, while first-order DHM time series only have negative generalized Hurst exponents. Different kind of auto-correlation in the series may account for this phenomenon. Although the basic statistical magnitudes of two series are similar, there is a big difference between the multifractality degree and time irreversibility. Therefore, MMRA provides another angle in describing the characteristics of time series.

3.3. Artificial time series based on the binomial multifractal model

In according with the binomial multifractal model [32], we construct the binomial multifractal series (*BMFs*) $\{x(i)\}$ with the length of $N = 2^{\max}$ in the following formula:

$$x_k = p^{n(k-1)}(1-p)^{n_{\max}-n(k-1)} \tag{13}$$

where $0 < p < 0.5$ is a parameter, $n(k)$ is the number of digits equal to 1 in the binary representation of index k. For example, $n(15) = 4$, since 15 corresponds to binary 1111. In our simulation, we generate series with length of $2^{13} = 8192$, with $p = 0.3$ for $\{x(i)\}$. Fig. 5 present time series generated from binomial multifractal model.

Here, we give some basic statistical magnitudes of time series generated from binomial multifractal model. The mean of the series is 1.2207e−004, the standard deviation of the series is 2.9617e−004 and the skewness is 10.1405.

In Fig. 6, we present the log–log plots of $MsAi_q$ vs. s for the time series generated from binomial multifractal model.

From Fig. 6, we can see that the value of $MsAi_q$ fluctuates between 0.2180 and 0.2657 and converges to 0.2500. Generally speaking, if $q < 0$, the fluctuation function $MsAi_q$ increases with the growth of the segment scale, while decreases with the growth of the segment scale if $q > 0$. If q takes the value of zero, the range of $MsAi_q$ is between 0.4949 and 0.5001. Since

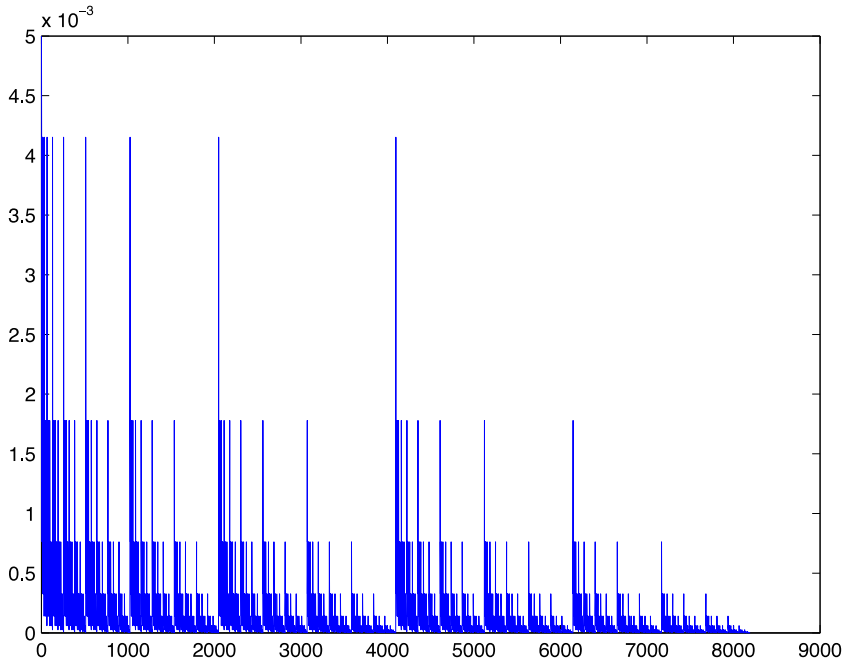

Fig. 5. Time series generated from binomial multifractal model.

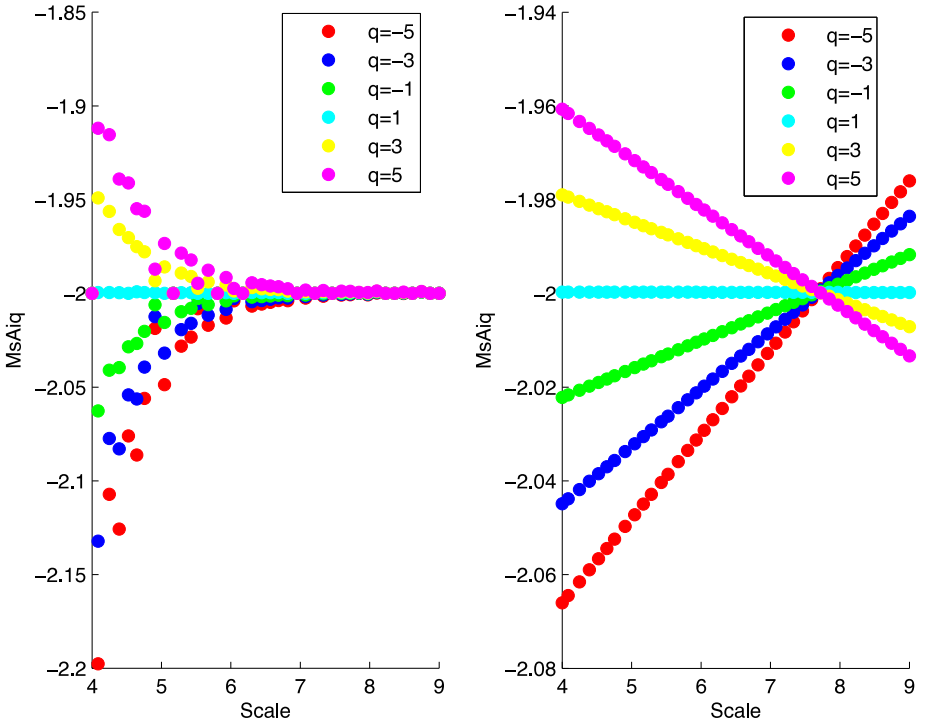

Fig. 6. The log–log plot of $MsAi_q$ vs. s of binomial multifractal series.

the case of $q = 0$ is different from other cases, we do not display the case of $q = 0$ in Fig. 6. For the same segment scale, the larger the value of q (except $q = 0$), the larger the value of fluctuation function $MsAi_q$. When the value of segment scale is large enough, the values of $MsAi_q$ tend to be same 0.2500. For different q and s, we have $MsAi_q \neq 0$, thus indicating that time series is irreversible. The scaling behavior of $MsAi_q$ is apparent and there is a significant dependence of $h(q)$ on q when the segment size $s \in \left(2^4, 2^6\right)$, which reveals the multifractality of time irreversibility of binomial multifractal series.

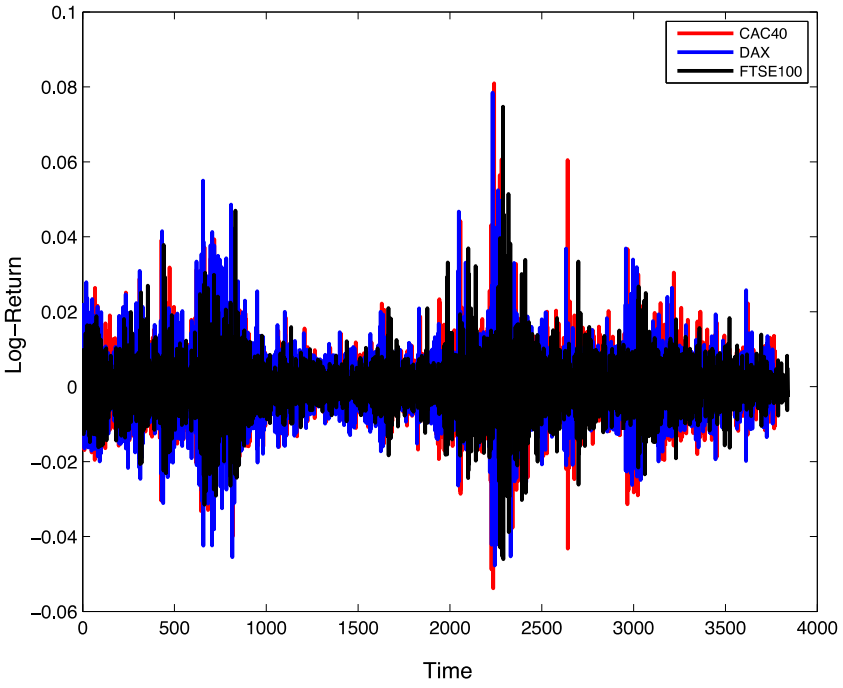

Fig. 7. The log-return of *CAC*40, *DAX* and *FTSE*100 Index in the Europe market.

Traditional multiscale time irreversibility analysis only reveal partial time irreversibility based on time delay. However, through the segmentation algorithm, MMRA analyzes the time irreversibility of every segment, which makes the time irreversibility of the series more elaborately and provides richer dynamic properties. This two kinds of artificial time series have proved the effectiveness of *MMRA* in assessing multifractality degree of multiscale time irreversibility and judging the fluctuation situation based on different statistical moments.

4. Empirical results

4.1. Empirical data

In this paper, we test for multiscale multifractal time irreversibility degree of 8 equity index returns in different regions. Let $\{x(t)\}$ be the equity index of a stock on a time t, the equity index returns, $r(t)$, are calculated as its logarithmic difference, $r(t) = \log[x(t+1)] - \log[x(t)]$. All data were collected from the Yahoo finance (http://finance.yahoo.com/). We choose three different regions in the world, Europe, Asia and US. In Europe, we have *CAC*40, *DAX*, *FTSE*100 Index. In Asia, we have *HangSeng*, *Nikkei*225, *SSE* Index, while in US, we have *Nasdaq*, *S*&*P*500 Index.

We employ daily data beginning in January 3, 2000 and ending in October 1, 2014. We have on average 3730 observations. The choice of the beginning of the series is due to our desire to study the stock market development in the 21st century. As far as we know, this is the first paper that utilizes multifractality in the study of multiscale time irreversibility in the stock markets. This is particularly meaningful, as it may provide guidance for the steady development of emerging market.

The graphical representation of returns of Europe, Asia, US are illustrated as Figs. 7, 8 and 9 respectively.

From Fig. 7, we can see the log-return of Europe market generally fluctuates around zero. There are two big fluctuations around 2003 and 2009, which reflects two financial crises in the 21st century. The impact of the latter one on Europe market seems to be far wider and more lasting than that of the former one. Among the three indices, *FTSE*100 Index undulates comparatively gentle, while *CAC*40, *DAX* Index is more acute.

HangSeng Index represents the situation of the emerging market, which tends to be more acute in comparison with Europe market, particularly between 2004 and 2007, which is a peaceful time for the global financial market. *SSE* Index and *Nikkei*225 Index are relatively stable in the 21st century.

From Fig. 9, we can see the log-return of US market generally undulates around zero. Similarly, there are two big fluctuations around 2003 and 2009, two financial crises in the 21st century may account for this phenomena. 2004–2007 is a shiny time for the US market. At the beginning of 21st century, *Nasdaq* Index waves intensively. With the passage of time, the two curves tend to overlap gradually.

The log-return plots only reveal superficial content of the stock market. In the following part, we will extract more information from the time irreversibility analysis of the log-returns.

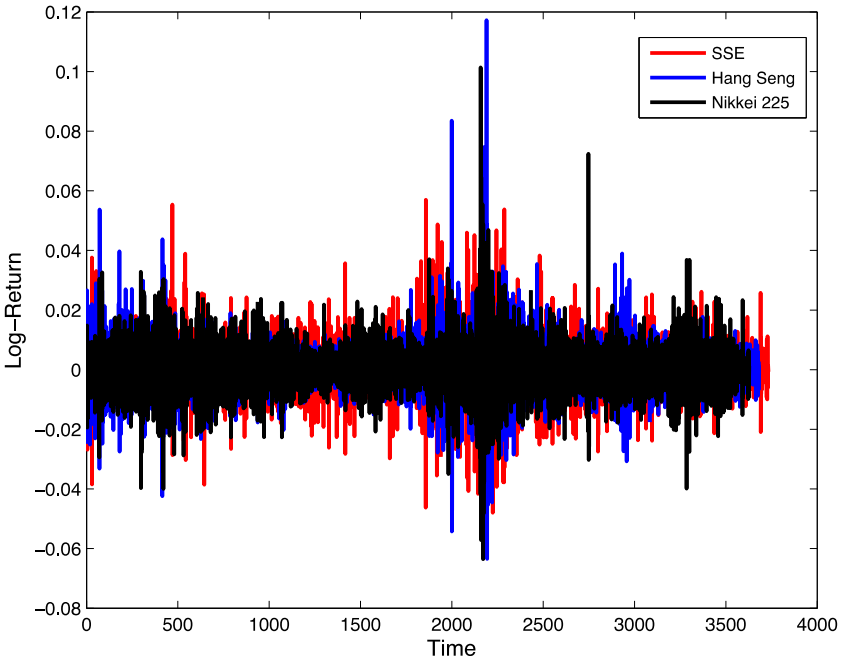

Fig. 8. The log-return of *SSE*, *HangSeng* and *Nikkei*225 Index in the Asia market.

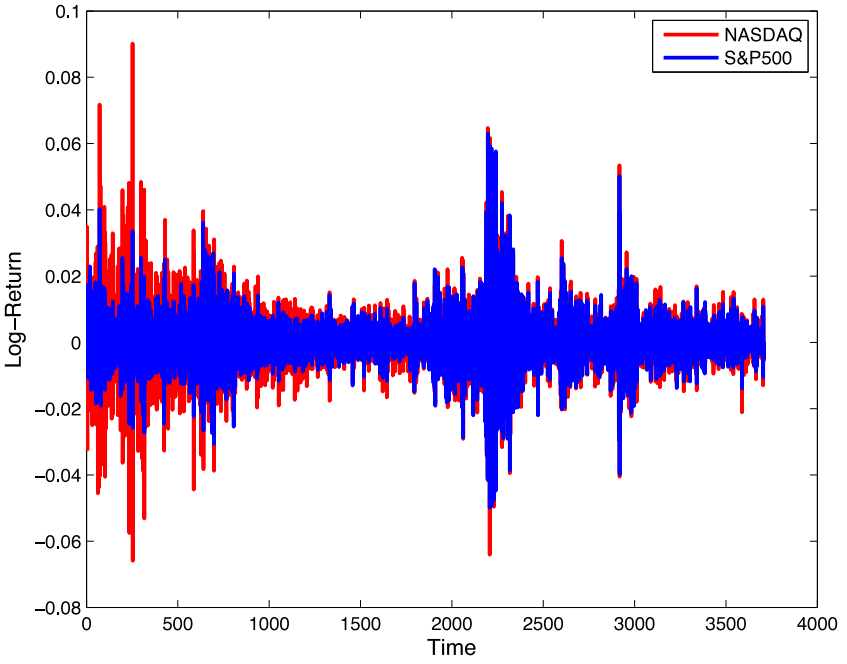

Fig. 9. The log-return of *S&P*500 and *Nasdaq* Index in the US market.

4.2. The multiscale multifractal time irreversibility of financial time series

Figs. 10–12 give the log–log plots of $MsAi_q$ vs. s for the stock indices (*CAC*40, *DAX*, *FTSE*100) of Europe market.

As we can see from Figs. 10–12, $MsAi_q$ decreases as the scale increases. That is to say, the more accurate the segment is, the more irreversible the sequence is. For negative q values, the power law between s and $MsAi_q$ is not very obvious. This may be induced by the large time irreversibility of the stock markets. Here, we present the linear fitting curve of $MsAi_q$. If $q = 0$, the time irreversibility is not apparently affected by the segment size. This means, in this case, $MsAi_q$ is constant whatever be s. For positive q values, the scaling behavior of the time irreversibility is significant. Furthermore, for the same

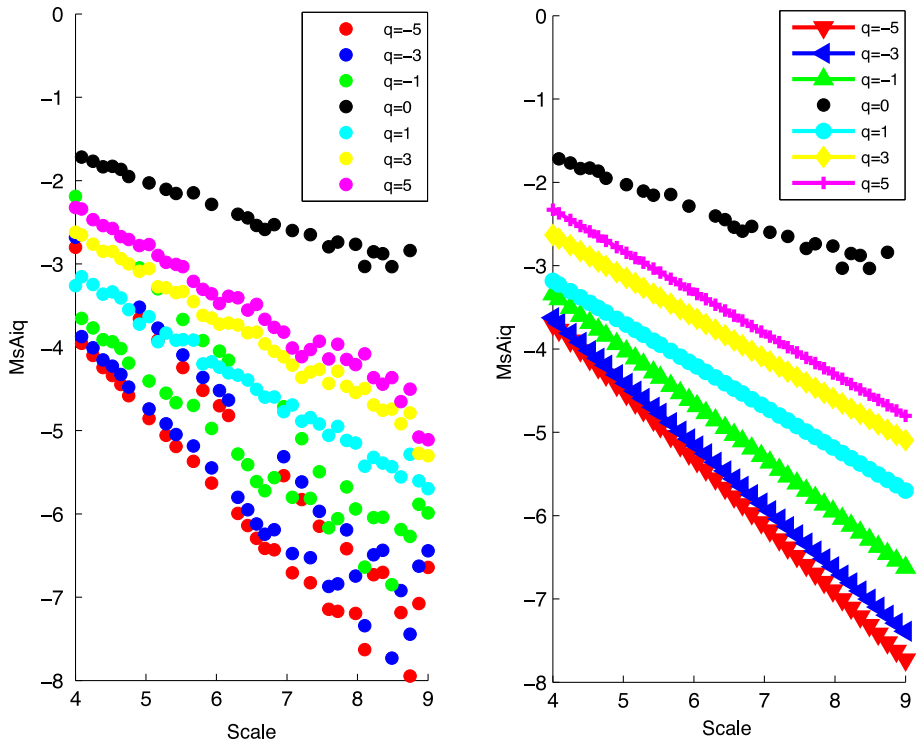

Fig. 10. The log–log plots of $MsAi_q$ vs. s for the CAC40 Index return with $q \in \{-5, -3, -1, 0, 1, 3, 5\}$. Note that there are two values for each window length s, one for the record starting from the beginning and the other from the record from the end. The generalized Hurst exponent obtained from the slope of the linear fit are $h(-5) = -0.8054$, $h(-3) = -0.7524$, $h(-1) = -0.6564$, $h(1) = -0.5037$, $h(3) = -0.4926$, $h(5) = -0.4946$.

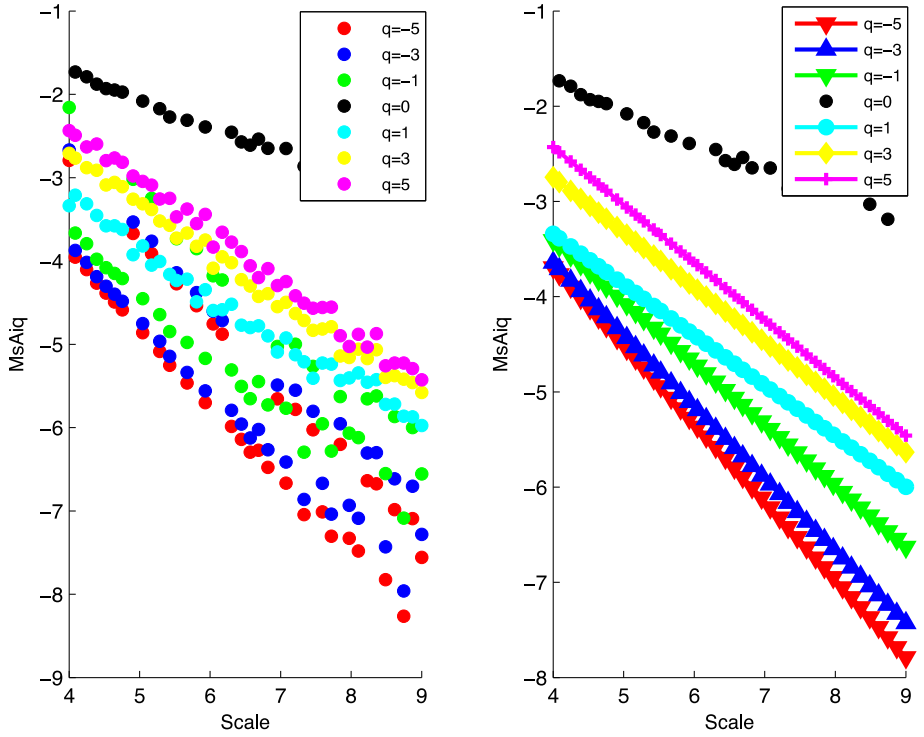

Fig. 11. The log–log plots of $MsAi_q$ vs. s for the DAX Index return with $q \in \{-5, -3, -1, 0, 1, 3, 5\}$. Note that there are two values for each window length s, one for the record starting from the beginning and the other from the record from the end. The generalized Hurst exponent obtained from the slope of the linear fit are $h(-5) = -0.8187$, $h(-3) = -0.7569$, $h(-1) = -0.6442$, $h(1) = -0.5312$, $h(3) = -0.5775$, $h(5) = -0.6056$.

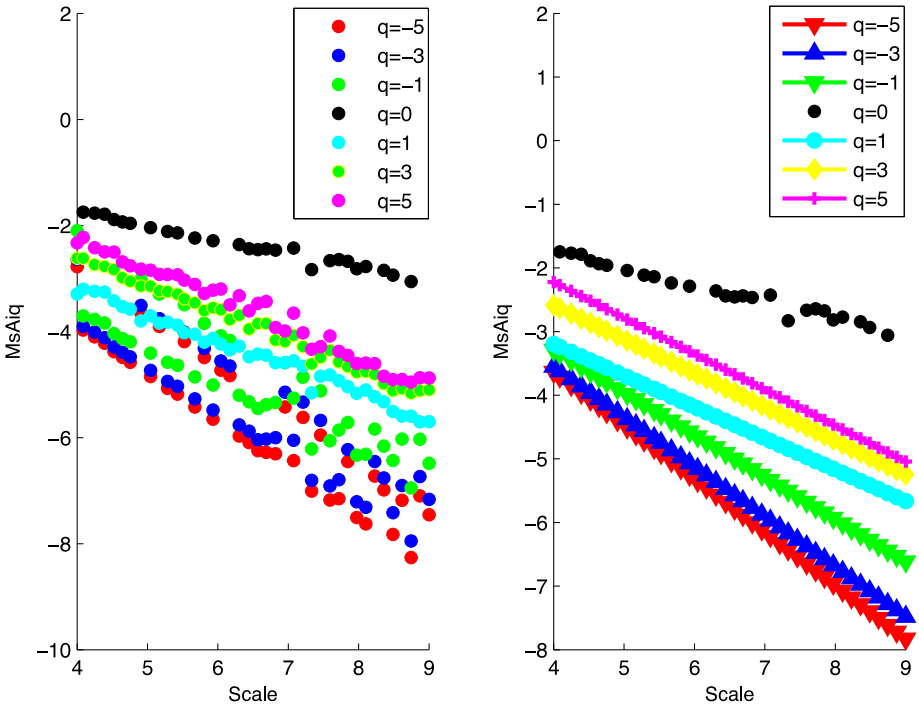

Fig. 12. The log–log plots of $MsAi_q$ vs. s for the FTSE100 Index return with $q \in \{-5, -3, -1, 0, 1, 3, 5\}$. Note that there are two values for each window length s, one for the record starting from the beginning and the other from the record from the end. The generalized Hurst exponent obtained from the slope of the linear fit are $h(-5) = -0.8384$, $h(-3) = -0.7860$, $h(-1) = -0.6653$, $h(1) = -0.4938$, $h(3) = -0.5322$, $h(5) = -0.5642$.

scale, $MsAi_q$ increases as the statistical moment increases. For negative q values, the generalized Hurst exponent fluctuates between -0.6442 and -0.8384 while for positive q values, the generalized Hurst exponent fluctuates between -0.6056 and -0.4926.

Figs. 13–15 give the log–log plots of $MsAi_q$ vs. s for the stock indices (*SSE*, *HangSeng*, *Nikkei*225) of Asia market.

On the whole, for negative q values, the generalized Hurst exponent fluctuates between -0.8753 and -0.6050. For positive q values, the generalized Hurst exponent fluctuates between -0.6286 and -0.4532. *HangSeng* Index's power law scaling behavior is more significant than *SSE* Index and *Nikkei*225 Index.

Figs. 16–17 display the log–log plots of $MsAiq(s)$ vs. s for the stock indices (*S&P*500, *Nasdaq*) of US market.

On the whole, for negative q values, the generalized Hurst exponent fluctuates between -0.8457 and -0.6945. For positive q values, the generalized Hurst exponent fluctuates between -0.6088 and -0.5368.

In the following part, we present the generalized Hurst exponent $H(q)$ vs. q in three different stock markets to dig more information.

From Figs. 18 and 19, we can see, for Europe market, the Hurst exponent of *CAC*40 index is similar to those of *DAX* and *FTSE*100 Index for the negative q, and for negative q, the Hurst exponent among three indices is *CAC*40 $>$ *FTSE*100 $>$ *DAX*; For Asia market, no matter what the value of q is, the Hurst exponent among three indices is *HangSeng* $>$ *Nikkei*225 $>$ *SSE*; For US Market, if $q < 1$, the Hurst exponent between two indices is *Nasdaq* $>$ *S&P*500, if $q > 1$, the Hurst exponent between two indices is *S&P*500 $>$ *Nasdaq*.

Generally, the absolute value of $h(q)$ of emerging market is lower than that of development market. As the market is becoming more and more mature, the time irreversibility of log-returns will become larger and larger.

5. Conclusions

In this paper, we have developed a method for the detection of multiscale time irreversibility and multifractality, which is called multiscale multifractal time irreversibility analysis (*MMRA*). This method is based on statistical moments. We applied MMRA to analyze the stock market indices.

This paper provides evidence that the multiscale multifractal time irreversibility for a broad range of stock markets is associated with the stage of their development. These results imply that multifractal multiscale time irreversibility may be used to assess stages of development.

The general Hurst exponent shows remarkable differences between developed and emerging markets, with high absolute values for the latter and low absolute values for the former. Therefore, our results are in accordance with previous findings. Furthermore, this connection can be considered a confirmation of the usefulness of the volatility.

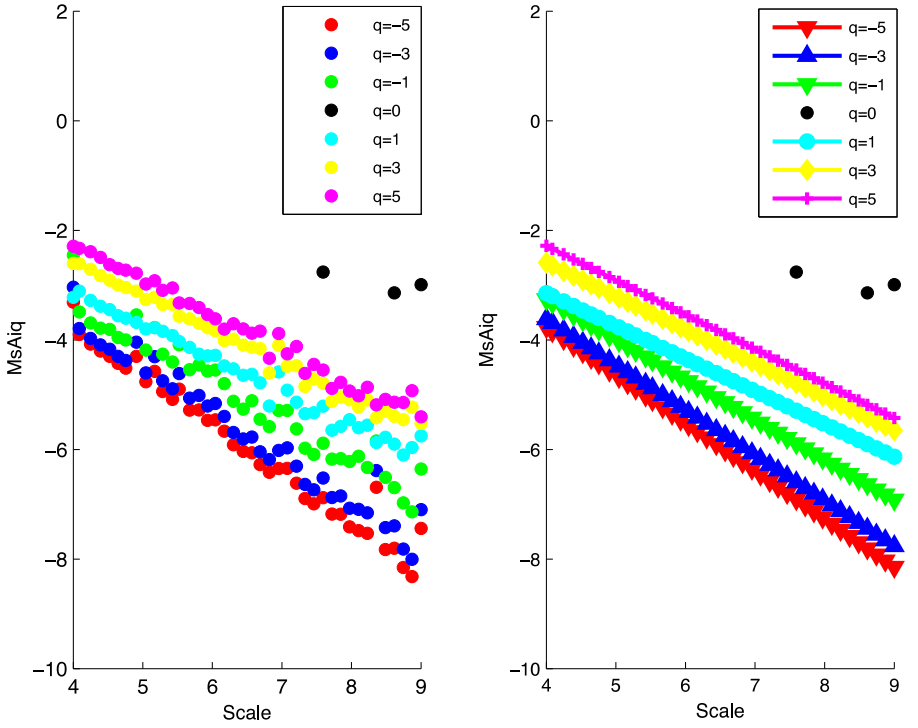

Fig. 13. The log–log plots of $MsAi_q$ vs. s for the *SSE* Index return with $q \in \{-5, -3, -1, 0, 1, 3, 5\}$. Note that there are two values for each window length s, one for the record starting from the beginning and the other from the record from the end. The generalized Hurst exponent obtained from the slope of the linear fit are $h(-5) = -0.8753$, $h(-3) = -0.8290$, $h(-1) = -0.7320$, $h(1) = -0.5966$, $h(3) = -0.6117$, $h(5) = -0.6286$.

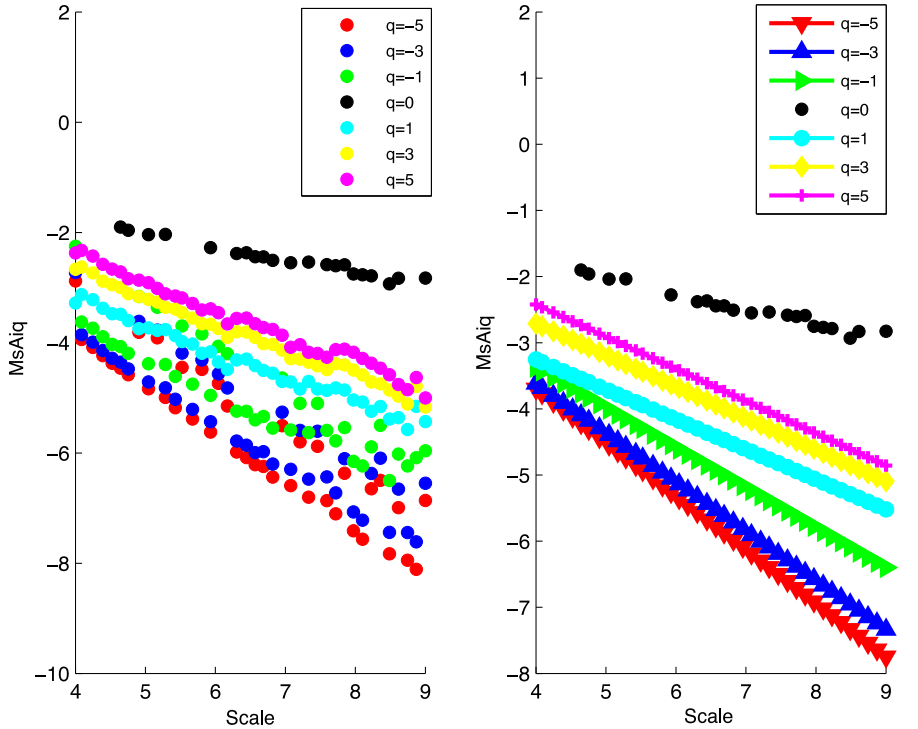

Fig. 14. The log–log plots of $MsAi_q$ vs. s for the *HangSeng* Index return with $q \in \{-5, -3, -1, 0, 1, 3, 5\}$. Note that there are two values for each window length s, one for the record starting from the beginning and the other from the record from the end. The generalized Hurst exponent obtained from the slope of the linear fit are $h(-5) = -0.8089$, $h(-3) = -0.7441$, $h(-1) = -0.6050$, $h(1) = -0.4532$, $h(3) = -0.4767$, $h(5) = -0.4871$.

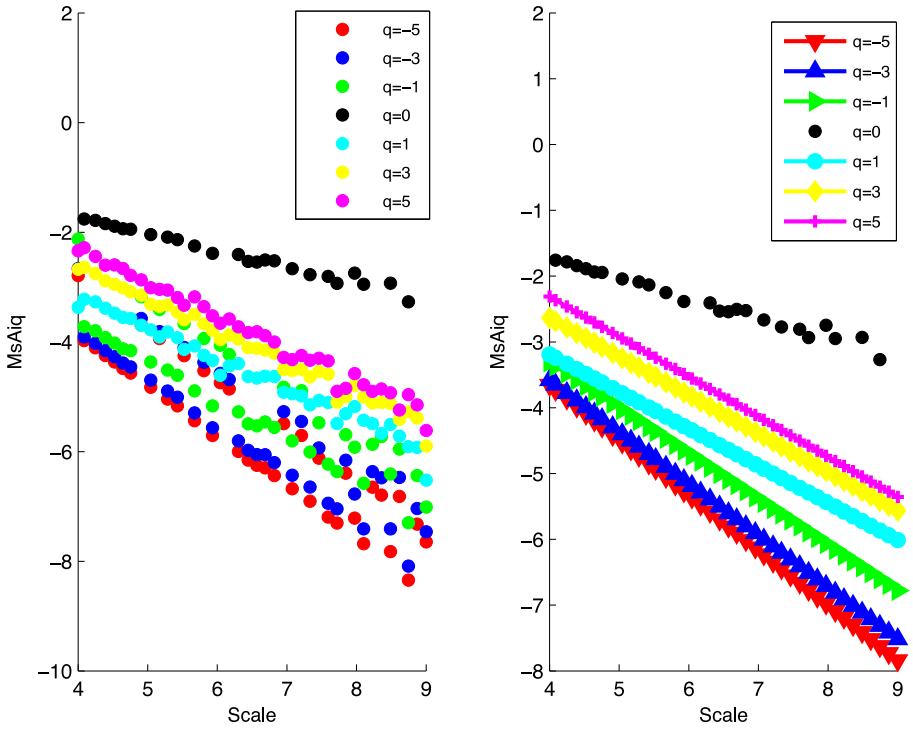

Fig. 15. The log–log plots of $MsAi_q$ vs. s for the *Nikkei*225 Index return with $q \in \{-5, -3, -1, 0, 1, 3, 5\}$. Note that there are two values for each window length s, one for the record starting from the beginning and the other from the record from the end. The generalized Hurst exponent obtained from the slope of the linear fit are $h(-5) = -0.8366$, $h(-3) = -0.7873$, $h(-1) = -0.6945$, $h(1) = -0.5638$, $h(3) = -0.5858$, $h(5) = -0.6088$.

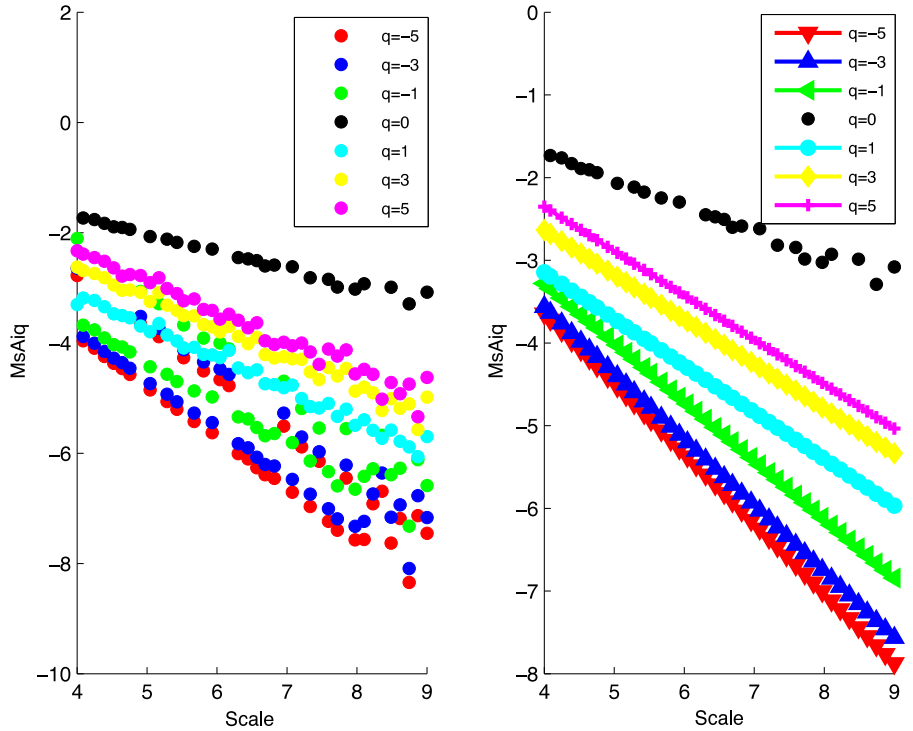

Fig. 16. The log–log plots of $MsAi_q$ vs. s for the *S*&*P*500 Index return with $q \in \{-5, -3, -1, 0, 1, 3, 5\}$. Note that there are two values for each window length s, one for the record starting from the beginning and the other from the record from the end. The generalized Hurst exponent obtained from the slope of the linear fit are $h(-5) = -0.8457$, $h(-3) = -0.8004$, $h(-1) = -0.7121$, $h(1) = -0.5645$, $h(3) = -0.5401$, $h(5) = -0.5368$.

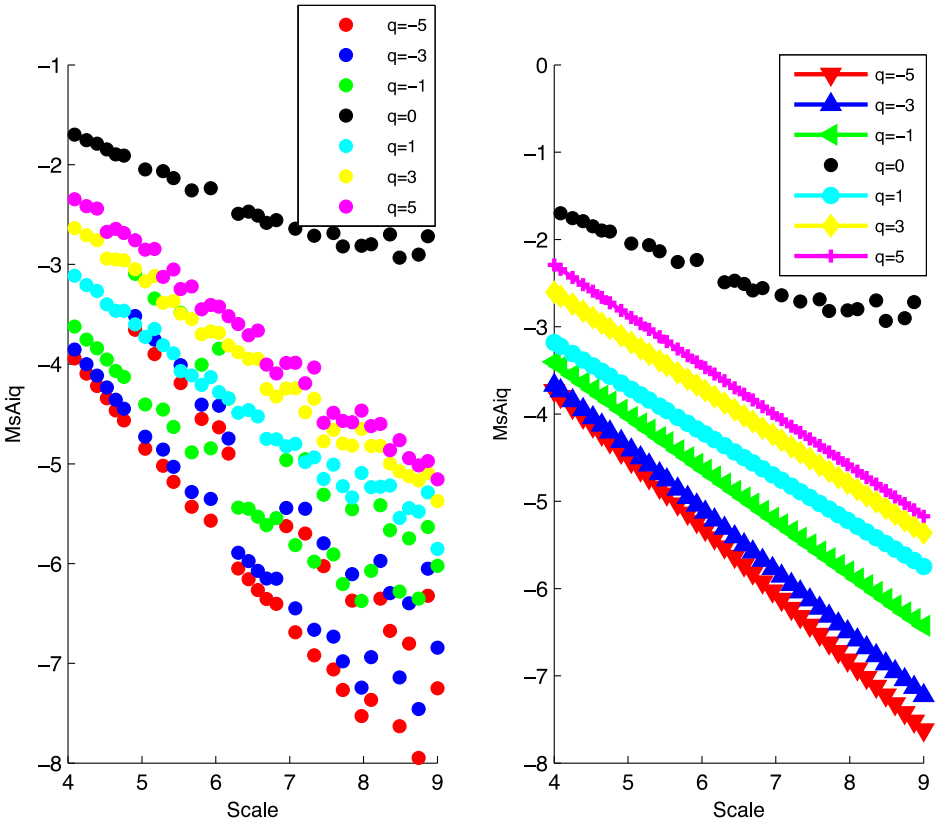

Fig. 17. The log–log plots of $MsAi_q$ vs. s for the *Nasdaq* Index return with $q \in \{-5, -3, -1, 0, 1, 3, 5\}$. Note that there are two values for each window length s, one for the record starting from the beginning and the other from the record from the end. The generalized Hurst exponent obtained from the slope of the linear fit are $h(-5) = -0.6580$, $h(-3) = -0.6115$, $h(-1) = -0.5218$, $h(0) = 0.0093$, $h(1) = -0.4255$, $h(3) = -0.4681$, $h(5) = -0.4952$.

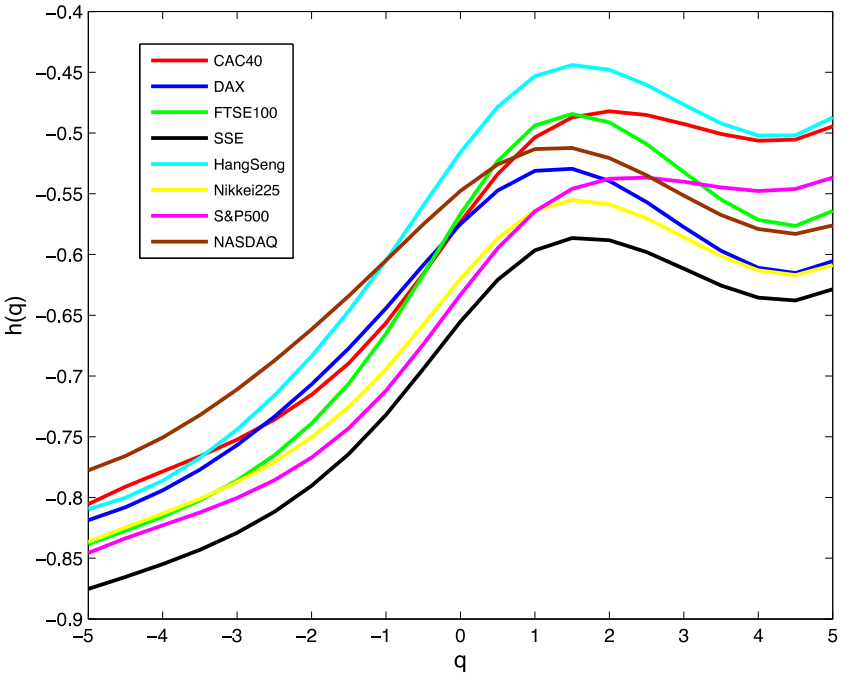

Fig. 18. Generalized Hurst Exponents $H(q)$ of different indices.

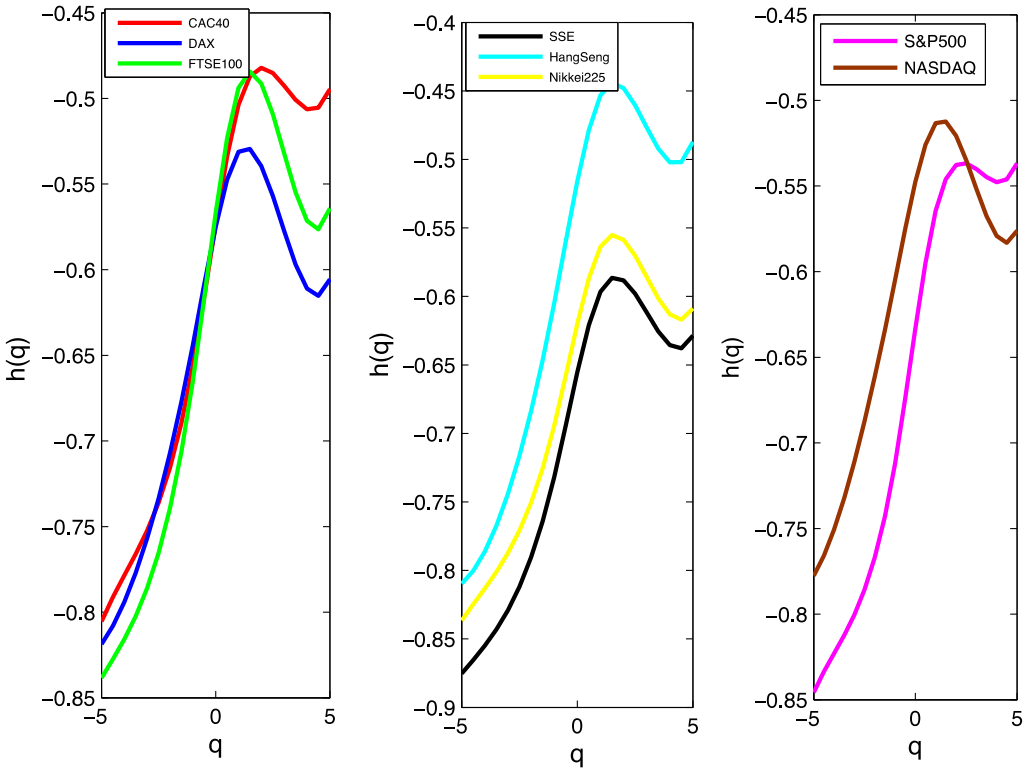

Fig. 19. Generalized Hurst Exponents $H(q)$ of three different regions.

Further research could exploit standard multiscale time irreversibility, based on time delay, segment size, statistical moments and study generalized Hurst surface, which could be used to characterize stock markets. Some emerging markets may be more developed than others, as they have dynamic and growing stock markets. Therefore, an ordered model could prove useful in this case.

Acknowledgments

Financial support by China National Science (61071142, 61371130), and Beijing National Science (4162047) is gratefully acknowledged.

References

[1] E.L. Siqueira, T. Stosic, L. Bejan, B. Stosic, Correlations and cross-correlations in the Brazilian agrarian commodities and stocks, Physica A 389 (14) (2010) 2739–2743.
[2] Y.D. Wang, L. Liu, R.B. Gu, J.J. Cao, H.Y. Wang, Analysis of market efficiency for the Shanghai stock market over time, Physica A 389 (2010) 1635–1642.
[3] M.Y. Bai, H.B. Zhu, Power law and multiscaling properties of the Chinese stock market, Physical A 389 (9) (2010) 1883–1890.
[4] L. Zunino, B.M. Tabak, A. Figliola, D.G. Perez, M. Garavaglia, O.A. Rosso, A multifractal approach for stock market inefficiency, Physica A 387 (26) (2008) 6558–6566.
[5] D.R. Cox, Long-range dependence,nonlinearity and time irreversibility, J. Time 12 (4) (1991) 329–335.
[6] A.J. Lawrence, Directionality and reversibility in time series, Internat. Statist. Rev. 59 (1) (1991) 67–69.
[7] M.B. Kennel, Testing time symmetry in time series using data compression dictionaries, Phys. Rev. E 69 (2004) 343–358.
[8] M.D. Costa, A.L. Goldberger, C.K. Peng, Broken asymmetry of the human heartbeat: loss of time irreversibility in ageing and disease, poster session three, J. Electrocardiol. 38 (2005) 140–144.
[9] A. Porporato, J.R. Rigby, E. Daly, Irreversibility and fluctuation theorem in stationary time series, Phys. Rev. Lett. 98 (9) (2007) 094101.
[10] C.K. Peng, S.V. Buldyrev, S. Havlin, M. Simons, H.E. Stanley, A.L. Goldberger, Mosaic organization of DNA nucleotides, Phys. Rev. E 49 (2) (1994) 1685–1689.
[11] N. Xu, P.J. Shang, S. Kamae, Minimizing the effect of exponential trends in detrended flutuation analysis, Chaos Solitons Fractals 41 (1) (2009) 311–316.
[12] B. Podobnik, H.E. Stanley, Detrended cross-correlation analysis:A new method for analyzing two non-stationary time series, Phys. Rev. Lett. 100 (8) (2008) 38–71.
[13] P.J. Shang, Y.B. Lu, S. Kamae, Detecting long-range correlations of traffic time series with multifractal detrended fluctuation analysis, Chaos Solitons Fractals 36 (1) (2006) 82–90.
[14] P.J. Shang, N. Xu, S. Kamae, Chaotic analysis of time series in the sediment transport phenomenon, Chaos Solitons Fractals 41 (1) (2009) 368–379.
[15] X.W. Li, P.J. Shang, Multifractal classification of road traffic flows, Chaos Solitons Fractals 31 (5) (2007) 1089–1094.
[16] Y. Yin, P.J. Shang, Asymmetric multiscale detrended cross-correlation analysis of financial time series, Chaos 24 (3) (2014) 032101–032101.
[17] K. Kiyono, Z.R. Struzik, N. Aoyagi, F. Togo, Y. Yamamoto, Phase transition in a healthy human heart rate, Phys. Rev. Lett. 95 (3) (2005) 058101.
[18] L.A.N. Amaral, P.C. Ivanov, N. Aoyagi, I. Hidaka, S. Tomono, A.L. Goldberger, H.E. Stanley, Y. Yamamoto, Behavioral-independent features of complex heartbeat dynamics, Phys. Rev. Lett. 86 (26) (2001) 6026–6029.

[19] D. Makowiec, R. Galaska, A. Dudkowska, A. Rynkiewicz, M. Zwierz, Long-range dependencies in heart rate signals-revisited, Physical A 369 (2) (2006) 632–644.
[20] H.E. Stanley, P. Meakin, Multifractal phenomena in physics and chemistry, Nature 335 (1988) 405–409.
[21] W.X. Zhou, Multifractal detrended cross-correlation analysis for two nonstationary signals, Phys. Rev. E 77 (6) (2008) 066211.
[22] M.R. Niu, W.X. Zhou, Z.Y. Yan, Q.H. Guo, Q.F. Liang, F.C. Wang, Z.H. Yu, Multifractal detrended fluctuation analysis of combustion flames in four-burner impinging entrained-flow gasifier, Chem. Eng. J. 143 (1–3) (2008) 230–235.
[23] R.B. Gu, H.T. Chen, Y.D. Wang, Multifractal analysis on international crude oil markets based on the multifractal detrended fluctuation analysis, Physica A 389 (14) (2010) 2805–2815.
[24] X.J. Zhao, P.J. Shang, A.J. Lin, G. Chen, Multifractal Fourier detrended cross-correlation analysis of traffic signals, Physica A 390 (2011) 3670–3678.
[25] P.J. Shang, S. Kamae, Fractal nature of time series in the sediment transport phenomenon, Chaos Solitons Fractals 26 (3) (2005) 997–1007.
[26] J. Wang, P.J. Shang, W.J. Ge, Multifractal cross-correlation analysis based on statistical moments, Fractals 20 (2012) 271–279.
[27] H.E. Stanley, V. Plerou, X. Gabaix, A statistical physics view of financial fluctuations: Evidence of scaling and universality, Physical A 387 (15) (2008) 3967–3981.
[28] V. Plerou, H.E. Stanley, Stock return distributions: tests of scaling and universality from three distinct stock markets, Phys. Rev. E 77 (2) (2008) 257–260.
[29] V. Plerou, H.E. Stanley, Tests of scaling and universality of the distributions of trade size and share volume: Evidence from three distinct markets, Phys. Rev. E 76 (2) (2007) 70–80.
[30] I. Prigogine, I. Antoniou, Laws of nature and time symmetry brearking, Ann. New York Acad. Sci. 879 (3528) (1999) 8–28.
[31] G. Weiss, Time-reversibility of linear stochastic processes, J. Appl. Probab. 12 (4) (1975) 831–836.
[32] H.o. Peitgen, H. Jurgens, D. Saupe, Chaos and Fractals, Springer, New York, 2008.